ISSN 1027-5495. Functional Materials, 23, No.4 (2016), p. 535-539.
doi:https://doi.org/10.15407/fm23.04.357

X-ray and photo-excited luminescence of $ZnWO_4$ nanoparticles with different size and morphology

I.A.Tupitsyna[1], *P.O.Maksimchuk*[1], *A.G.Yakubovskaya*[1], *Y.V.Malyukin*[1], *V.S.Zvereva*[1], *O.M.Vovk*[2]

[1] Institute for Scintillation Materials, STC "Institute for Single Crystals", National Academy of Sciences of Ukraine, 60 Nauky Ave., 61001 Kharkiv, Ukraine
[2]Institute for Single Crystals, STC "Institute for Single Crystals", National Academy of Sciences of Ukraine, 60 Nauky Ave., 61001 Kharkiv, Ukraine

Received September 12, 2016

X-ray and photoluminescence of $ZnWO_4$ nanocrystals with controlled size and morphology: grains with diameter of 10–20 nm; rods with diameter of 10–20 nm and length of 200–250 nm produced by microwave hydrothermal method were studied. Red luminescence with λ_{max} = 700 nm was found in the samples. The intensity of the red luminescence increases with decreasing of the $ZnWO_4$ nanoparticles size due to increase of concentration of oxygen vacancies and creation of distorted WO_6 centers. It was shown that reduction in the X-ray luminescence intensity with decrease of the $ZnWO_4$ nanoparticles size is due to creation of the distorted WO_6 centers which are the nonradiative relaxation channel competing with the self-trapped excitons.
Keywords: nanocrystals, $ZnWO_4$, oxygen vacancies, luminescence, scintillator.

Исследована рентгено- и фотолюминесценция нанокристаллов $ZnWO_4$ с контролируемыми размерами и морфологией: зерна диаметром 10–20 нм; стержни диаметром 10–20 нм и длиной 200–250 нм, полученные гидротермально-микроволновым методом. В исследованных образцах обнаружена красная люминесценция с λ_{max} = 700 нм, интенсивность которой растет с уменьшением размера наночастиц $ZnWO_4$, что обусловлено увеличением концентрации вакансий кислорода и созданием искаженных WO_6 центров. Показано, что снижение интенсивности рентгенолюминесценции при уменьшении размера наночастиц $ZnWO_4$ связано с конкурирующим с автолокализованным экситоном безызлучательным каналом релаксации — искаженными WO_6 центрами.

Рентгено- та фотолюмінесценція наночастинок $ZnWO_4$ різних розмірів і морфології. *І.А.Тупіцина, П.О.Максимчук, Г.Г.Якубовська, Ю.В.Малюкін, В.С.Звєрєва, О.М.Вовк.*

Досліджено рентгено- та фотолюмінесценцію нанокристалів $ZnWO_4$ з контрольованими розмірами та морфологією: зерна діаметром 10–20 нм; стрижні діаметром 10–20 нм і довжиною 200–250 нм, отримані гідротермально-мікрохвильовим методом. У досліджених зразках виявлено червону люмінесценцію з λ_{max} = 700 нм, інтенсивність якої зростає зі зменшенням розміру наночастинок $ZnWO_4$, що обумовлено збільшенням концентрації вакансій кисню і створенням спотворених WO_6 центрів. Показано, що зниження інтенсивності рентгенолюмінесценції при зменшенні розміру наночастинок $ZnWO_4$ пов'язано з конкуруючим з автолокалізованим екситоном безвипромінювальним каналом релаксації — спотвореними WO_6 центрами.

1. Introduction

Zinc tungstate single crystals are known as scintillators for tomography, dosimetric and spectrometric systems used for radiation monitoring, digital radiography, as well as for registration of the rare nuclear events [1–3]. Scintillation materials based on $ZnWO_4$ attract special attention because its parameters are close to such of cadmium tungstate, however, they have low level of radioactivity and are non-toxic on its own [2].

Preparation of nanoscale scintillators based on divalent metal tungstate is actual problem [4–7]. It was developed due to prospective use of inorganic nanoscintillators with a large effective atomic number in medicine and biology for photodynamic therapy [8, 9]. A recent approach relies on use of the scintillating nanoparticles that upon exposure to ionizing radiation, such as X-rays, emit luminescence in the visible region, which, in turn, activates a conjugated photosensitizer through the Forster resonance energy transfer (FRET) [10–15]. X-ray inducible photodynamic therapy has practically no limitation in the penetration depth in tissues. Another advanced application of the nanoscintillators which stimulates its studies is the development of X-ray fluorescence imaging [16–18]. For this purpose, besides increasing of the penetration depth, the known effect of selective accumulation of the nanoparticles in tumor cells is used.

A number of papers relating to the scintillation properties of particles of submicron and nanoscale size in comparison with the bulk crystals describe changes of the material properties due to size reduction [19–21]. This effect is attributed to a change in defects of the crystal structure [19]. The method of modeling of recombinational luminescence intensity dependence on the nanoparticle size is proposed on the basis of assumption that contribution to the recombinational luminescence gives only those charge carriers which in a result of thermalization did not reach a near-surface layer of the nanoparticles [21].

It was shown that X-ray luminescence intensity decreases with decrease of $ZnWO_4$ nanoparticles size [22,23]. For understanding of nature of this effect the luminescent properties of $ZnWO_4$ nanoparticles of different size and morphology before and after annealing in oxygen atmosphere have been investigated in this paper.

Table. The impurity composition of starting materials

	$Zn(NO_3)_2$, ppm	Na_2WO_4, ppm
Fe	2.5	≤5
Mn	1	≤5
Mg	5	≤5
Pb	10	≤1
Cr	2	≤5
Cu	<0.2	≤5
Sn	1	≤0.5
Ni	1	≤1
Mo	1	≤1

2. Experimental

We used the following starting materials: $Na_2WO_4 \cdot 2H_2O$, $Zn(NO_3)_2 \cdot 6H_2O$ (impurity composition is shown in Table 1), $NH_3 \cdot H_2O$ of analytical grade purity (98 %).

Synthesis of nanoparticles was carried out in two stages. Initially, amorphous $ZnWO_4$ was prepared by co-precipitation of 25 ml 0.1 M aqueous solutions of $Zn(NO_3)_2$ and Na_2WO_4 at the room temperature with vigorous stirring. pH of the solutions was adjusted by adding dilute aqueous 30 % $NH_3 \cdot H_2O$ solutions. The synthesis was carried out by microwave hydrothermal method on microwave installation MARS (GEM Corporation Matthews, USA) at temperature of 120, 200°C and frequency of 2.45 GHz for 30 min. Upon completion of the synthesis the white precipitate was filtered, washed with distilled water and dried at 70°C in air for 3 h.

Annealing of the nanocrystals was carried out in air at temperature of 400°C for 12 h. This temperature was selected because increasing of grain size was observed at the temperatures higher than 500°C [24].

X-ray phase analysis of the samples was characterized by X-ray powder diffraction (XRD) on Siemens D 500 powder diffractometer (radiation $CuK\alpha$, nickel filter, Bragg-Brentano geometry).

Morphology of the nanocrystals was investigated by transmission electron microscopy using EM-125 (SELMA, Ukraine) microscope. Electron accelerating voltage was 125 kV, the survey was carried out in the bright field mode, and the image was recorded by CCD matrix.

Luminescence spectra of the nanocrystals were recorded by means of automatic spectrofluorimeter based on the lattice mono-

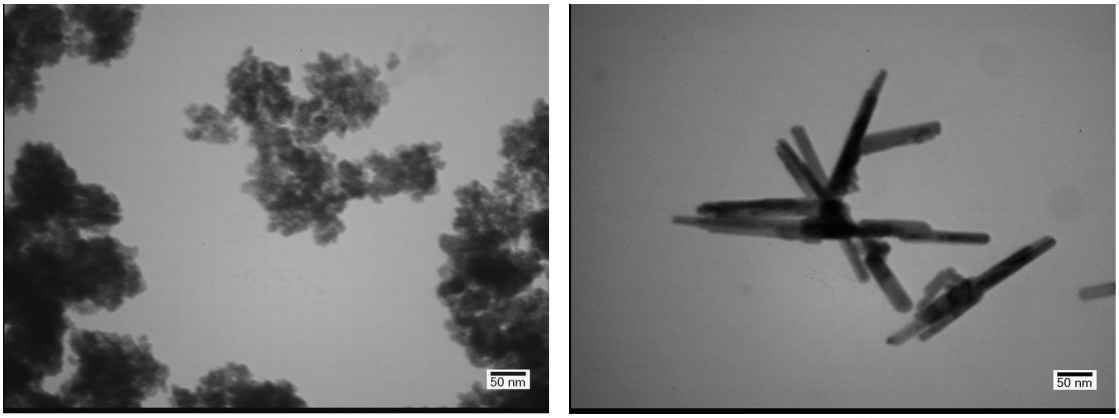

Fig. 1. TEM image of $ZnWO_4$ nanoparticles obtained by microwave hydrothermal method: (a) — grains (pH = 9.5, T = 120°C); (b) — rods (pH = 9.5, T = 200°C).

chromator MDR-23. Photomultiplier Hamamatsu R9110 operating in the photon counting mode was used for luminescence spectra registration. The 3-rd and the 4-th radiation harmonics of YAG:Nd laser (λ_{ex} = 266 nm and 355 nm) were used as the photoluminescence excitation sources. X-ray generator REYS (U_α = 25 kV, i_a = 0.37 μA) was used as an X-ray excitation source.

3. Results and discussion

Structure of obtained $ZnWO_4$ powders was monoclinic (wolframite). TEM images are shown in Fig. 1. We obtained $ZnWO_4$ with grains size of 10–20 nm (further called the "grains") synthesized under pH = 9.5, T = 120°C conditions. Rods of 10–20 nm in diameter and length of 200–250 nm, referred to as the "rods", were prepared at pH = 9.5 and T = 200°C.

The luminescence spectra of investigated powders under X-ray excitation at the room temperature are broad asymmetric bands with a maximum at 495–500 nm (Fig. 2). This glow is typical for the bulk $ZnWO_4$ crystals. It is connected with radiative relaxation of excitation of oxyanion complex WO_6^{6-} with electron transfer from 5*d* W on 2*p* O, traditionally described as a relaxation of the self-trapped exciton [25–27]. Luminescence of the "grains" is insignificant (Fig. 2, cr. *1*), while the "rods" have intense glow, practically unchanged after annealing in air (Fig. 2, cr. *3* and *4*). The intensity of the "grains" luminescence after annealing in air is greatly increased (Fig. 2, cr. *2*).

The measurements of the $ZnWO_4$ nanoparticles photoluminescence spectra (after annealing) under excitation with λ_{ex} = 266 nm correspond to band with λ_{max} = 470 nm for the "grains" and "rods", due to

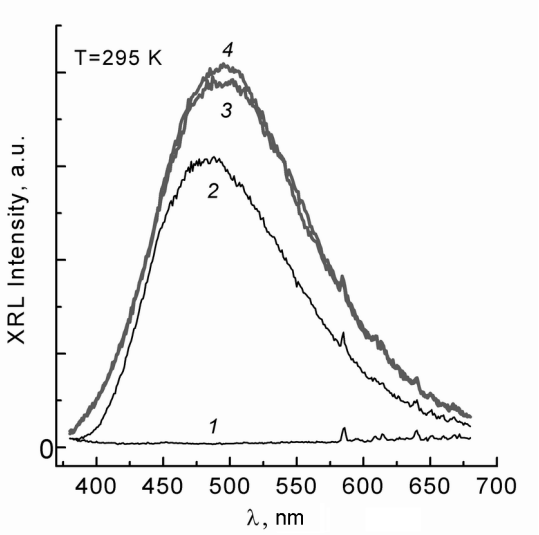

Fig. 2. X-ray luminescence of nanoparticles $ZnWO_4$: *1* — grains, *2* — grains after annealing, *3* — rods, *4* — rods after annealing.

relaxation of the self-trapped exciton, the same as for X-ray excitation (Fig. 3). Under the "rods" excitation at λ_{ex} = 355 nm in addition to the basic glow at λ_{max} = 470 nm the broad band luminescence at λ_{max} = 700 nm of the same intensity was observed (Fig. 3, a). For the "grains" the contribution of red band with λ_{max} = 700 nm is much greater under the excitation at λ_{ex} = 355 nm (Fig. 3, b). The both "grains" and "rods" the red luminescence band intensity at the room temperature is low, but the glow becomes brighter by almost 2 orders of magnitude if the temperature is lowered to 80 K.

Investigation of effect of annealing of the "grains" in oxygen atmosphere by the red luminescence showed that after the annealing in air the intensity of luminescence

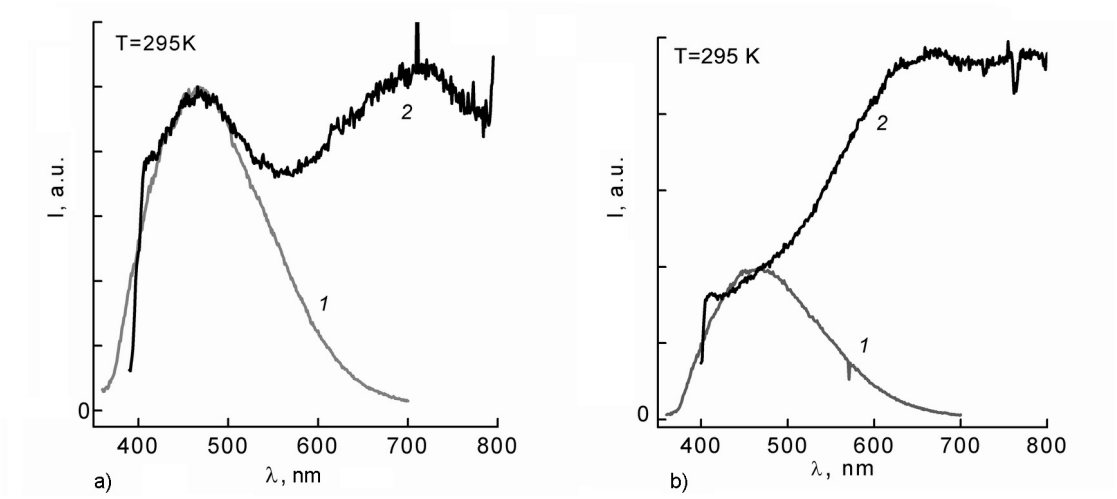

Fig. 3. Normalized photoluminescence spectra of $ZnWO_4$ nanoparticles after annealing (a) rods, (b) grains under excitation: *1* — λ_{ex} = 266 nm, *2* — λ_{ex} = 355 nm.

band of λ_{max} = 700 nm decreased by a factor of 2 (Fig. 4).

Reducing of the baseband X-ray intensity (λ_{max} = 495 nm) as the size of the nanoparticles decrease (at the same time the intensity of the red luminescence band with λ_{max} = 700 nm increases) caused by increasing luminescence centers concentration competing with the glow of the self-trapped excitons. The luminescence of impurities as observed for the bulk crystals $ZnWO_4$:Mo [28] can not occur for our samples because investigated samples have low content of the impurities, in particular Mo less than 1 ppm.

The results allow us to conclude that the red luminescence with λ_{max} = 700 nm is more intense for $ZnWO_4$ "grains" and it is associated with oxygen vacancies. This is consistent with the known data for other nanoparticles of inorganic oxide compounds: as nanoparticles size decrease (due to the larger surface deposit) the concentration of the oxygen vacancies increases. In particular, fluorescent techniques shows that reduction of CeO_2 nanocrystals size (from 75 to 20 nm) leads to increase by 1.5 times the band luminescence of Ce^{3+} stabilized by the oxygen vacancies, whereas CeO_2:Eu^{3+} downsizing leads to symmetry reduction of Eu^{3+} [29]. Also for these nanocrystals extremely high concentrations of the oxygen vacancies and hence Ce^{3+} ions were determined by EPR — 44 % for 3 nm size nanoparticles and 17 % for 30 nm [30, 31].

WO_3 monophasic samples were investigated by G.Blasse [32]. The crystalline structure of WO_3 relates to perovskite-like compounds containing octahedra with a central ion with d^0 configuration. Their luminescence is described by the wide band with λ_{max} = 700 nm and its intensity is considerably reduced at the higher temperatures. Similar spectral data were obtained for luminescence complex $[W_{10}O_{32}]^{4-}$ [33]. Luminescence of these compounds attributed to transitions with charge transfer in WO_6-octahedra, the structural parameters of which (the distance W–O, angles) differ from those of $ZnWO_4$.

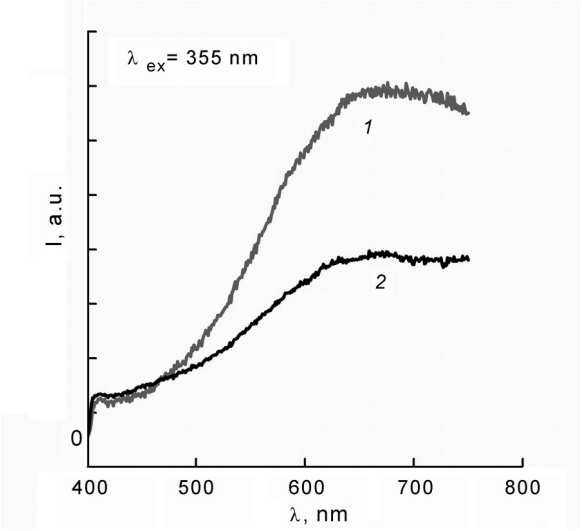

Fig. 4. Photoluminescence spectra of $ZnWO_4$ nanoparticles under excitation λ_{ex} = 355 nm: *1* — grains, *2* — grains after annealing.

In $ZnWO_4$ nanocrystals due to high concentration of the oxygen vacancies, which increases with decreasing the particle size, the WO_6-octahedra with a distorted structure close to the structure of WO_3 octahedra can form. Annealing in the oxygen atmosphere leads to healing the oxygen vacancies,

decreasing of the lattice distortion and reducing the red emission intensity. The luminescence of such distorted WO_6-octahedra can be described as luminescence of centres with a low probability of emission. Under photoexcitation with energy corresponding to excitation of the luminescence centre, we provide the situation of the most favorable excitation and observe the most intensive emission at the low temperatures. Probability of the radiative relaxation decreases with increasing the temperature due to increasing of the electron-phonon interaction. Under the X-ray excitation the red luminescence was not observed even in the sample with a high concentration of the oxygen vacancies. In this case the distorted WO_6 centers appear as a competing nonradiative relaxation channel and luminescence intensity of the main bands decreases.

4. Conclusions

$ZnWO_4$ nanocrystals with controlled size and morphology were obtained by microwave hydrothermal method: grains with diameter of 10–20 nm; rods with diameter of 10–20 nm and a length of 200–250 nm.

The luminescence with $\lambda_{max} = 700$ nm, the intensity of which increases with decreasing of the $ZnWO_4$ nanoparticles size due to increase of oxygen vacancies and creation of distorted WO_6 centers was observed.

It was shown that the decrease of the X-ray luminescence intensity with the $ZnWO_4$ nanoparticle size decreasing is due to the non-radiative relaxation channel — distorted WO_6 centres which are competing with the self-trapped excitons.

References

1. M.Globus, B.Grinyov, J.K.Kim, Inorganic Scintillators for Modern and Traditional Applications, Institute for Single Crystals, Ukraine, Kharkiv (2005).
2. L.L.Nagornaya, B.V.Grinyov, A.M.Dubovik et al., *IEEE Trans. Nucl. Sci.*, **56**, 994 (2009).
3. R.Shi, Y.Wang, D.Li et al., *Appl. Catal. B: Environ*, **100**, 173 (2011).
4. H.M.Shang, M.Bliss, S.Heald et al., *J. Mater. Res.*, **22**, 1527 (2007).
5. H.M.Shang, Y.Wang, M.Bliss et al., *Appl. Phys. Lett.*, **87**, 051909 (2005).
6. S.H.Yu, M.Antonietti, H.Colfen, M.Giersig, *Angew. Chem. Int. Ed. Engl.*, **41**, 2356 (2002).
7. A.G.Yakubovskaya, K.A.Katrunov, I.A.Tupitsyna et al., *Functional Materials*, **18**, 446 (2011).
8. P.Retif, S.Pinel, M.Toussaint et al., *Theranostics*, **5**, 1030 (2015).
9. A.-L.Bulin, A.Vasil'ev, A.Belsky et al., *Nanoscale*, **7**, 5744 (2015).
10. K.Kirakci, P.Kubat, K.Fejfarova, *Inorg. Chem.*, (2015) doi: 10.1021/acs.inorgchem.5b02282
11. S.S.Lucky, K.C.Soo, Y.Zhang, *Chem. Rev.*, **115**, 1990 (2015).
12. W.Chen, J.J.Zhang, *J. Nanosci. Nanotechnol.*, **6**, 1159 (2006).
13. A.-L.Bulin, C.Truillet, R.Chouikrat et al., *J. Phys. Chem. C*, **117**, 21583 (2013).
14. Y.Tang, J.Hu, A.H.Elmenoufy et al., *ACS Appl. Mater. & Interfaces*, **7**, 12261 (2015).
15. H.Chen, G.D.Wang, Y.-J.Chuang et al., *J. Nano Lett.*, **15**, 2249 (2015).
16. Z.Yi et al., *Biomater. Sci.*, **2**, 1404 (2014).
17. Y.Yang, *Biomaterials*, **34**, 774 (2013).
18. L.Rao, *J. Mater. Chem. B*, **2**, 6527 (2014).
19. L.Wang, Y.Ma, H.Jiang, *J. Mater. Chem. C*, **2**, 4651 (2014)
20. A.V.Ishchenko, R.F.Samigullina, T.I.Krasnenko et al., *Radiat. Measur.* (2016), doi: 10.1016/j.radmeas.2016.01.030
21. V.Vistovskyy, Ya.Chornodolskyy, A.Gloskovskii et al., *Radiat. Measur.*, **90**, 174 (2016).
22. A.Yakubovskaya, I.Tupitsyna, D.Sofronov et al., *Functional Materials*, **20**, 523 (2013).
23. V.M.Lisitsyn, D.T.Valiev, I.A.Tupitsyna et al., *J. Lumin.*, **153**, 130 (2014).
24. A.Kalinko, A.Kuzmin, *J. Luminescence*, **129**, 1144 (2009).
25. V.Nagirnyi, E.Feldbach, L.Jonsson et al., *Nucl. Instr. and Meth. Phys. Res. A*, **486**, 395 (2002).
26. Cz.Koepke, A.Lempicki, *J. Luminescence*, **59**, 33 (1994).
27. H.Kraus, V.B.Mikhailik, Y.Ramachers et al., *Phys. Lett. B*, **610**, 37 (2005).
28. N.R.Krutyak, V.V.Mikhailin, A.N.Vasil'ev et al., *J. Luminescence*, **144**, 105 (2013).
29. P.O.Maksimchuk, V.V.Seminko, I.I.Bespalova et al., *Functional Materials*, **21**, 254 (2014).
30. P.Dutta, S.Pal, M.S.Seehra et al., *Chem. Mater.*, **18**, 5144 (2006).
31. U.Deshpande, S.Patil, S.Kuchibhatla et al., *Appl. Phys. Lett.*, **87**, 133113:1-3 (2005).
32. G.Blasse, M.Wiegel, *J. Alloys Comp.*, **224**, 342 (1995).
33. T.Yamase, M.Sugeta, *J. Chem. Soc., Dalton Trans.*, 759 (1993).